Referee #2 Evaluations:

Reviewer #2 (Formal Review for Author):

General comments:

The paper considers about two hundred events of quasi-monochromatic atmospheric gravity waves (QMGWs) which were acquired over five years of observations in Southern Brazil, obtained with an OH all-sky imager. Gravity waves exhibited a seasonal dependence on the propagation direction with an anisotropic behavior. Typical characteristics of QMGWs are horizontal wavelengths of 10 - $55\,\text{km}$, observed periods of $5 - 74$ minutes and observed phase speeds up to $100\,\text{m/s}$. A complimentary backward ray tracing analysis allowed the authors to reveal potential sources of QMGWs. I have found the paper to be interesting to the atmospheric community. At the same time, there are issues that are needed to explain and clarify. This is why a revision of the present paper is needed.

Specific comments

The authors would like to thank the reference for taking time off to review this manuscript and for the comments, suggestions, and corrections. We have given the response accordingly.

- **Lines 2 - 3:** "The observations were made using OH all-sky imagers hosted by the Southern Space Observatory (SSO)..."

    Question: How many all-sky imagers were used? One or several?

    Response: Gravity wave observations were taken at the Southern Space Observatory (SSO), located in São Martinho da Serra (SMS) (29.44°S; 53.85°W), Rio Grande do Sul, Brazil, using a single-filter (OH) imager that began operation from April 2017 till date.

    Based on this comment, the entire Section on OH All-Sky Imager. See **Line 41 - 51** in the revised manuscript.

- **Lines 46 - 48**: "Details on the observation mode (including the temporal resolution and integration time) and production of the final image can be seen elsewhere in Bageston et al. (2009) and Nyassor et al. (2021, 2022)."

    Question: Temporal and horizontal spatial resolutions are not "details" but the main parameters of the instrument, which should be presented here.

    Response: Based on your comment, the entire section of the all-sky imager and the observation mode has been written all over in the main text as shown in the red highlighted text below:

This imager is equipped with a Charge Coupled Device (CCD) camera (SBIG, STL-1001E model), which has a resolution of 1024×1024 pixels, each pixel measuring $24.6 \times 24.6\,\mu$m, and 50% of quantum efficiency in the near-infrared spectrum. The image was not binned but cropped to 512×512 pixels, producing a final image size of 12×12 mm on the CCD chip with a spatial resolution of 512×512 km. Each image has an integration time of 20 s and a readout time of 10 s, since the imager does not have a filter wheel, the temporal resolution is 38 seconds (Bageston et al., 2009; Nyassor et al., (2021,2022)). Airglow observations were taken when the Sun and Moon elevations were lower than -12° and 10°, respectively. This mode allows 28 nights of observation per month, centered on the new moon.

This text can be seen on **Line 41 - 51** in the revised manuscript.

- **Line 66-67**: "Afterward, the images are unwarped and mapped into the geographical coordinates." It is unclear how were images mapped into the geographic coordinates? In order to do it, one needs to make a total geometrical calibration (not only the alignment of the original airglow image to the geographical north) but solving the optical model of the camera for EACH pixel. A brief procedure of the geometrical calibration for each pixel is needed here.

- **Lines 76-77:** "Figure 1. Flowchart showing the procedures of airglow image processing and wave parameter estimation. The three stages describe image preprocessing and processing, spectral analysis, and wave parameters estimation procedure." In the flowchart and in section 3 "Methodology and Data Analysis", I cannot see removals of the atmospheric background (not atmospheric extinction) and noise level of the sensor. Also, there is no information on the flat field correction of the sensor. How these issues have been treated in the image processing? These should be described.

  Response: Due to your comment, the entire section of the methodology has been written all over the main text, as shown in the red highlighted text below:

  Linear wave patterns in original all-sky airglow images appear curved due to curvature effects projected by the fisheye lens. Also, all-sky images contain stars during clear sky conditions. Therefore, it is important to preprocess the images before determining the spectral characteristics of the observed waves. The image preprocessing and spectral analysis procedure adapted in this work follows the approach of Garcia et al. (1997) and Wrasse et al. (2007).

  The preprocessing begins with the alignment of the original airglow image to the geographical north (also called standard coordinate). Original all-sky images depict an array of data recorded by the CCD camera of i and j coordinate axes, with each point in the array representing a pixel index in the data array. These axes are not aligned with a specific geographic orientation. Therefore, a linear transformation of the original image coordinates is scaled so that the horizon circle that corresponds to 0° elevation is of unit radius (Hapgood et al., 1982). The final geographic coordinate system is a 2-D uniformly spaced grid at the height of the airglow layer such that the zenith is located at the origin of the coordinate system and the x and y axes correspond to geographic east and north, respectively. Next, the geometric calibration was carried out. This is achieved by using the determined position of the stars in the original all-sky image and the positions of stars in the sky maps, considering the image time and the latitude and longitude of the site.

Stars present steaking when the image is unwrapped. Also, they exhibit sharp, localized changes in intensity, whereas airglow exhibits much more gradual changes. So, these sharp changes due to the stars are determined and replaced with interpolated values from the surrounding pixels. However, if the intensity changes exceed a certain threshold, the intensity is scanned until it returns to within a threshold of the background. On the contrary, it is considered too large to be a star, and thus it is disregarded.

The intensity of airglow observed by a ground-based imager is not uniform due to varying zenith angles, even for a spatially uniform airglow emission. The observed intensity is proportional to the length of the line of sight (LOS) in the airglow emission layer, known as the van Rhijn effect. Also, the amount of atmospheric absorption is proportional to the length of the LOS from the emission layer to the observation point. This atmospheric absorption, known as atmospheric extinction, weakens the observed airglow intensity. The Van Rhijn effect and atmospheric extinction were corrected by applying the method of Kubota et al. (2001).

To finally get the image in a form for spectral analysis to be applied, the image must be unwarped. First, the lens function (which varies in angle from the center to the edge of the image) determined during the geometric calibration was used to perform an interpolation for a geographical grid. The procedure is repeated for each point in the geographical grid to obtain the unwarped image. Afterward, the fluctuation fraction (flat fielding) of the intensity of the unwarped images is carried out to investigate relative intensity variations in the airglow. The fluctuation fraction provides a relative percentage measure of how much the intensity of a given pixel varied in a given instant. The fraction calculation of the intensity fluctuation is determined using Equation 1 (Garcia et al., 1997):

$$\frac{\delta I}{\bar{I}} = \frac{I - \bar{I}}{\bar{I}} \tag{1}$$

where I represents the luminous intensity contained in any image of the night sky and $\bar{I}$ is the average image of the whole night. To reduce the effect of the background atmosphere, the average of the entire night of observation is computed and subtracted from the individual images of the night. Also, to reduce the noise level of the sensor, an image is taken at the start of the observation with the shutter closed. This is done to determine the approximate noise of the system. The image preprocessing, spectral analysis and estimation of the gravity wave parameters are summarized in a flowchart in Figure 1. For more details on the airglow image preprocessing, see Garcia et al. (1997).

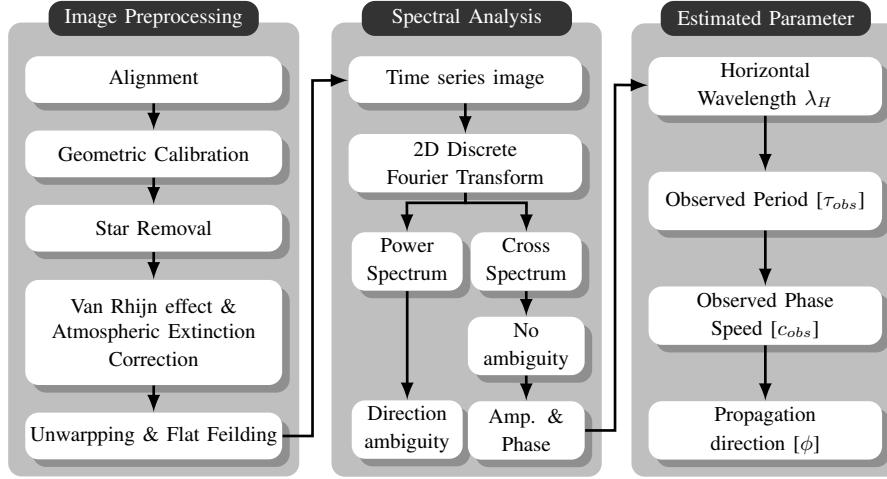This text can be seen on **Line 61 - 97** in the revised manuscript as well as the revised Flowchart.

Figure 1: Flowchart showing the procedures of airglow image processing and wave parameter estimation. The three stages describe image preprocessing and processing, spectral analysis, and wave parameters estimation procedure.

- Before presenting statistical results, it is worth presenting a figure demonstrating an example of an observed quasi-monochromatic gravity wave.

  Response: The figure of the observed QMGWs and keogram presented in the main text is shown below.
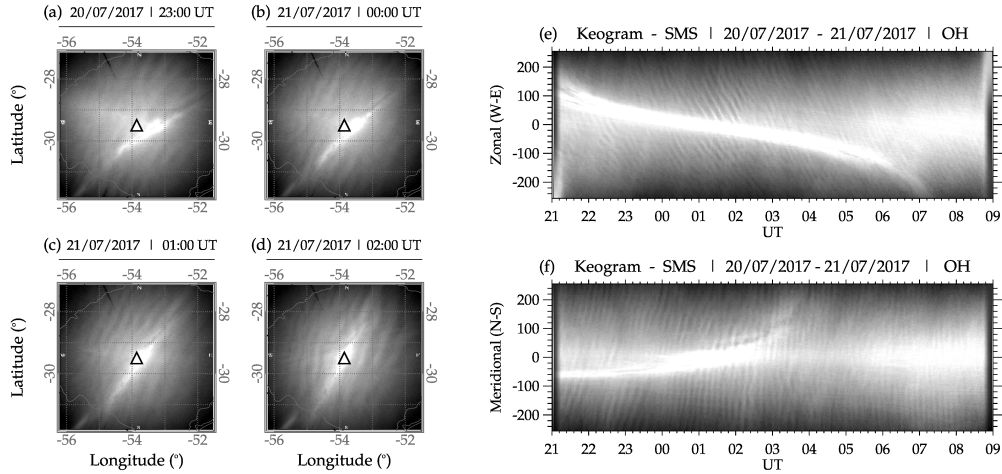

Figure 2: The observed quasi-monochromatic gravity wave (QMGW) on July 20 to 21 2017 at São Martinho da Serra.

Below is the description of the 2 as it is in the revised manuscript:

In Figure 2, a sample of four preprocess images at 23:00:01 UT, 00:00:49 UT, 01:00:16 UT and 02:01:04 UT plotted on the geographic map is presented in panels (a), (b), (c), and (d), respectively. The white triangle with a black outline shows the center of the all-sky image and the location of the imager. The gray lines in panels (a), (b), (c), and (d) depict the state borders of Rio Grande do Sul. The bright strand extending from the southwest through the center of the image to the northeast is the

4

Milky Way. In the keogram, the Milky Way is the white strand extending through the middle throughout the observation. It is important to mention that the keograms presented here are only used to show the presence of the QMGWs throughout the observation time from 21:00 UT on July 20th to 09:00 UT on 21st. It can be seen that the wave packet changes with time from the northwest to the southwest. An animation of the propagation of the 20-21, 2017 QMGW event between 21:00 UT on July 20 2017 and 09:00 UT on July 21, 2017 is provided in the video supplement. In panels (e) and (f), the zonal and meridional components of the keogram, where a downward phase progression of black and white undulations can be seen in the zonal component. The black and white vertical undulations have an upward phase progression in the meridional component of the keogram. This clearly shows the presence of a quasi-monochromatic structure throughout the night.

- Something is wrong with the caption on the horizontal axis of Fig. 3c.

  Response: The caption of Figure 3c (now 4c) has been corrected and the caption of entire figure has been revised as shown below:

  Quasi-Monochromatic Gravity Waves (QMGWs) characteristics over five years of observations at São Martinho da Serra. Panels (a), (b), and (c) present the histogram of the horizontal wavelength (λ_H), period (τ_H), and phase speed (c_H), respectively. In panel (d), the propagation direction (ϕ) of the QMGWs are presented according to season.

  See Figure 4 and Caption on page 9 of the revised manuscript.

- **Line 153-154:** "Similarly, most waves observed in the OH airglow images were visible and propagated for 2-3 hours."

  Question: I do not understand this definition "duration of propagation of the waves in the OH images´´. Does it mean that an observed wave package (a number of wave crests and troughs) did propagate for 2-3 hours in the field of view of the imager? Or is it something else? This should be explained.

  Response: We meant to say observed wave packet (a number of wave crests and troughs) did propagate for 2-3 hours across the field of view of the imager as you rightly said. So, according to your comment, the text below has been added for clarification.The new added texts are in blue.

  The propagation time of the waves from their source to the observation altitude in the mesosphere is presented in Figure 6(a), while the duration of propagation (thus the time span the propagating waves were visible in the OH images during the night) of the waves in the OH images is presented in Figure 6(b). It can be seen that the majority of the wave propagated less than one hour from the source position in the lower atmosphere to the OH emission layer. Similarly, the observed wave packet from which the individual QMGWs were selected in the OH airglow images were visible over the field of view of the all-sky imager and propagated for 2-3 hours.

  See Line 196 - 197 and Line 198 - 200 of the revised manuscript for this chanages.

- **Lines 406-407:** "Also, Mastrantonio et al. (1976) showed that the gravity waves generated by tropospheric jet streams may have the ability to propagate vertically to the upper atmosphere, such as the ionosphere (Mastrantonio et al., 1976).´´

Here it is worth citing two more papers:

Dalin et al. (2015) demonstrated a particular transient isolated gravity wave in the summer mesopause associated with the passage of an occluded front and/or the point of occlusion. The mechanism of the wave generation was likely due to strong horizontal wind shears at about 5 km altitude. Dalin et al. (2016) demonstrated that gravity waves, observed in the summer mesopause, were associated with the upper tropospheric jet stream at altitudes 8 – 10 km.

Additional references:

Dalin, P., A. Pogoreltsev, N. Pertsev, V. Perminov, N. Shevchuk, A. Dubietis, M. Zalcik, S. Kulikov, A. Zadorozhny, D. Kudabayeva, A. Solodovnik, G. Salakhutdinov, I. Grigoryeva: Evidence of the formation of noctilucent clouds due to propagation of an isolated gravity wave caused by a tropospheric occluded front. Geophysical Research Letters, 42, 2037-2046, doi:10.1002/2014GL062776, 2015.

Dalin, P., N. Gavrilov, N. Pertsev, V. Perminov, A. Pogoreltsev, N. Shevchuk, A. Dubietis, P. Völger, M. Zalcik, A. Ling, S. Kulikov, A. Zadorozhny, G. Salakhutdinov, and I. Grigoryeva: A case study of long gravity wave crests in noctilucent clouds and their origin in the upper tropospheric jet stream. Journal of Geophysical Research - Atmospheres, 121, doi:10.1002/2016JD025422, 2016.

Response: Thanks very much. The references has been in cited in the revised manuscript as shown below:

Using two synchronized automated digital cameras at Krasnogorsk and Obninsk, located near Moscow, Russia, Dalin et al. (2015) demonstrated that a particular transient isolated gravity wave in the summer mesopause is associated with the passage of an occluded front and/or the point of occlusion. The source mechanism of the wave generation, according to Dalin et al. (2015), was likely due to strong horizontal wind shears at about 5 km altitude. Similarly, Dalin et al. (2016) illustrated that gravity waves, observed in the summer mesopause, were associated with the upper tropospheric jet stream at altitudes 8 – 10 km.